JOURNAL OF NATURAL PRODUCTS

Article

pubs.acs.org/jnp

Terms of Use

Synthetic Chondramide A Analogues Stabilize Filamentous Actin and Block Invasion by *Toxoplasma gondii*

Christopher I. Ma,[†] Karthikeyan Diraviyam,[‡] Martin E. Maier,[§] David Sept,[‡] and L. David Sibley*[,†]

[†]Department of Molecular Microbiology, Washington University School of Medicine, St. Louis, Missouri 63110, United States

[‡]Department of Biomedical Engineering and Center for Computational Medicine and Bioinformatics, University of Michigan, Ann Arbor, Michigan 48109, United States

[§]Institut für Organische Chemie, Universität Tübingen, 72076 Tübingen, Germany

Supporting Information

ABSTRACT: Apicomplexan parasites such as *Toxoplasma gondii* rely on actin-based motility to cross biological barriers and invade host cells. Key structural and biochemical differences in host and parasite actins make this an attractive target for small-molecule inhibitors. Here we took advantage of recent advances in the synthesis of cyclic depsipeptide compounds that stabilize filamentous actin to test the ability of chondramides to disrupt growth of *T. gondii in vitro*. Structural modeling of chondramide A (**2**) binding to an actin filament model revealed variations in the binding site between host and parasite actins. A series of 10 previously synthesized analogues (**2b**–**k**) with substitutions in the β-tyrosine moiety blocked parasite growth on host cell monolayers with EC_{50} values that ranged from 0.3 to 1.3 μM. *In vitro* polymerization assays using highly purified recombinant actin from *T. gondii* verified that synthetic and natural product chondramides target the actin cytoskeleton. Consistent with this, chondramide treatment blocked parasite invasion into host cells and was more rapidly effective than pyrimethamine, a standard therapeutic agent. Although the current compounds lack specificity for parasite vs host actin, these studies provide a platform for the future design and synthesis of synthetic cyclic peptide inhibitors that selectively disrupt actin dynamics in parasites.

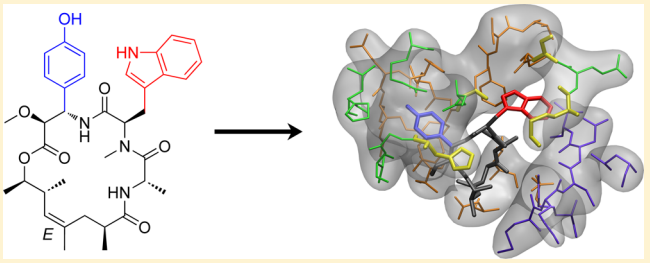

Toxoplasma gondii is a widespread parasite of animals that often results in zoonotic infections in humans, of which ~25% show serological evidence of chronic infection.[1] In humans, *T. gondii* exists either as rapidly growing tachyzoites that predominate during normally short-lived acute infections or as cyst-forming bradyzoites, which are found during chronic infection and capable of causing reactivation. Congenitally infected infants suffer a variety of sequelae from mild to severe illness,[2] and immunocompromised individuals such as patients undergoing chemotherapy or organ transplant are vulnerable to the reactivation of toxoplasmosis.[3] HIV patients are also at risk of *T. gondii*-induced encephalitis,[4] especially where highly active antiretroviral therapy (HAART) remains underutilized.[5−10] Finally, *T. gondii* is a frequent infectious cause of ocular disease, especially in some regions of Brazil.[11−13] Current therapeutics such as pyrimethamine and sulfadiazine do not clear latent infection of the parasite and are often not tolerated due to allergic reactions, illustrating the need for better drugs.[14]

T. gondii is an obligate intracellular parasite, similar to other medically important apicomplexans such as *Plasmodium* spp., the cause of malaria, and *Cryptosporidium parvum*, which causes diarrheal disease. A potential target in apicomplexans is the actin cytoskeleton, which plays an important role in parasite motility and invasion into host cells.[15] Although entry is largely driven by the parasite, the host cytoskeleton also participates in this process,[16] likely as a scaffold for anchoring adhesins involved in parasite invasion.[17] Studies in *Plasmodium* support a similar important role for parasite actin dynamics in cell invasion,[18] although *T. gondii* remains the model for the phylum due to its ease of use for cellular, biochemical, and molecular studies. Actin in *T. gondii* is ~80% identical to host actin, and yet these proteins exhibit key structural and biochemical differences.[19,20] Apicomplexans utilize a simplified set of regulatory proteins such as actin depolymerizing factor (ADF) and profilin, both of which largely function to sequester monomeric actin.[20−23] A similar repertoire of actin-binding proteins is found in *Plasmodium*,[24] highlighting the conservation of actin dynamics among this group. Unlike mammalian cells or yeast, the majority of actin in *T. gondii*[25] or *Plasmodium falciparum*[26] remains in an unpolymerized form or in very short filaments, and yet motility requires the polymerization of actin filaments (F-actin).[15,27] The unconventional properties of *T. gondii* actin compared to mammalian actins, combined with its important role in host cell invasion, suggest that inhibitors that disrupt actin dynamics in the parasite might prevent infection.

A number of natural products disrupt actin dynamics including phalloidins that stabilize F-actin by binding to a

Received: March 7, 2013
Published: September 10, 2013

ACS Publications © 2013 American Chemical Society and American Society of Pharmacognosy

specific site in the filament.[28] Although phalloidins are highly toxic due to their ability to cause muscle rigor, they are not readily cell permeant, thus limiting their utility as a scaffold for generating selective inhibitors. In contrast, a number of cell-permeant cyclic depsipeptides also act to stabilize F-actin. Jasplakinolide (**1**), originally isolated from the marine sponge *Jaspis johnstoni*,[29] induces polymerization and binds to F-actin to stabilize the filament.[30,31] In *T. gondii*, **1** induces aberrant growth of stable actin filaments and disrupts gliding motility and cell entry at submicromolar concentrations.[32−34] Jasplakinolide (**1**) has fungicidal and antitumor activity;[35−38] however, it also disrupts actin networks in normal mammalian cells,[39] thus limiting the therapeutic potential of this molecule. Recent identification of novel jasplakinolide analogues[40] may ultimately provide compounds that are selective; however, identifying natural compounds requires isolation, structural characterization, and purification of sufficient quantities for testing, which may limit the potential range of molecules that can be obtained by this route.

Chondramides, natural cyclodepsipeptides isolated from myxobacteria, are structurally similar to **1**, with an 18-membered instead of 19-membered macrocyclic ring.[29,41,42] Chondramides A−D (**2**−**5**) block growth of yeasts and are cytostatic to cultured animals cells.[43] The complete chemical synthesis and compound derivatization have been investigated based on **2** and **4** scaffolds, allowing generation of a number of structurally related analogues.[44−47] Taking advantage of these developments, we previously reported schemes for efficient chemical synthesis of **2** as a means of generating increased diversity of chondramides, and these compounds were shown to disrupt actin and inhibit mammalian cell division.[45,47] In the present study, we compared the activities of natural compounds **2**−**4** as well as 10 previously described synthetic analogues (**2b**−**k**) for their ability to stabilize F-actin *in vitro* and block infection of *T. gondii in vitro*. Although the compounds tested here do not show selectivity for parasite over host actin, they nonetheless are potent inhibitors of parasite invasion and provide useful leads for future development of more specific compounds.

RESULTS AND DISCUSSION

Modeling of Chondramide A (2) Binding to F-Actin. Previous studies have predicted that **1** binds at the interface of three monomers in the F-actin filament, stabilizing it against turnover and disrupting actin dynamics in the parasite.[20] Computational modeling of **2** was used to compare the binding pocket in F-actin and to examine potential differences between host and parasite actins. To account for filament flexibility, which is not captured in standard docking calculations, we performed a molecular dynamics simulation and used a series of muscle F-actin poses to dock **2** using Glide (Schrödinger LLC, New York, NY, USA). The optimal binding conformation for muscle actin was also used to build a homology model for the *T. gondii* actin filament that was then docked with **2** (Figure 1A). Compound **2** was predicted to bind at the interface of three monomeric actin subunits of the filament (Figure 1B, Figure S1), similar to the binding site previously proposed for **1**[20] and overlapping with the previously identified binding site for phalloidin, a competitive filament-stabilizing compound.[20]

The predicted binding conformation for **2** differs from that proposed previously for **4**,[46] which was based on an earlier, lower resolution F-actin model.[48] In that prior study, the authors favored a pose where the OH of the *β*-tyrosine moiety

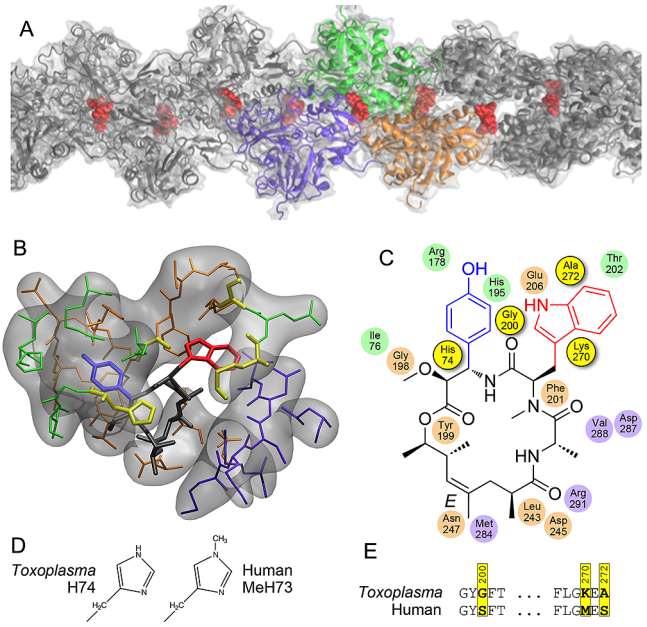

Figure 1. Predicted binding site for chondramide in the actin filament. (A) Molecular docking of chondramide A (**2** shown in red) to a homology model of *T. gondii* F-actin identifies the binding site at the interface of three protomers (orange, green, purple). (B) Enlarged view of the three protomers that make up the binding site, which are shown in green, orange, and purple with residues within 4.0 Å highlighted. (C) Regions of contact that differ between human and parasite actins are shown in yellow in the 2D representation of the binding site. (D) Histidine is methylated in mammalian actin. (E) Sequence alignment indicating the residue differences between parasite and mammalian actin.

of **4** points toward Thr202 in actin, while in our model, this region of **2** fits in a different pocket lined by Arg178, Asp179, and Gly200 (numbering based on *T. gondii* actin), and instead, the indole ring of the *N*-methyl-D-tryptophan points toward Thr202 (Figure 1B,C). This prior study also gave preference to the phalloidin binding conformation in choosing the final conformation for **4**. Although phalloidin and chondramides bind to a similar overall site in the actin filament, they differ structurally, and hence we did not impose this constraint in our docking of **2**. Several improvements in the present study likely account for the differences in the predicted binding sites, including the use of a higher resolution F-actin model[28] and a more exhaustive combination of docking and molecular dynamics, which allows a consensus docking site to be determined from a series of poses.

Detailed analysis of the chondramide binding site in actin (Figure 1A,B, Figure S1) identified several residues that are different between *T. gondii* and muscle (Figure 1C−E). There are two variable residues in actin that are in close proximity (<5 Å) to the OH group of the *β*-tyrosine of **2**: Gly200, which corresponds to Ser199 in muscle, and His74, which is methylated-His73 in muscle (highlighted in yellow, Figure 1C,D). The related parasite *Plasmodium* lacks this modification,[26] suggesting it may be absent in apicomplexans. Consistent with this, LC-MS/MS analysis of actin purified from *T. gondii* showed no evidence for methylation of His74 (Figure 2A), although this modification was detected in TgACTI (*T. gondii* actin) that was expressed and purified from baculovirus (Figure 2B). The absence of methylation of His74 in actin expressed by the parasite is expected to change

dx.doi.org/10.1021/np400196w | J. Nat. Prod. 2013, 76, 1565−1572

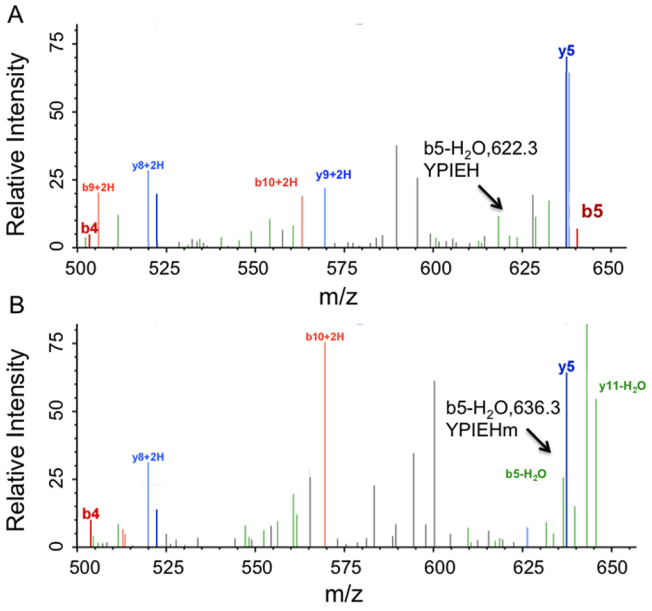

Figure 2. Analysis of peptide mass fingerprint of TgACTI tryptic digest by LC-MS mass spectrometry. (A) The *m/z* spectrum of the peptide YPIEHGIVTNWDDMEK indicates that actin immunoprecipitated from *T. gondii* shows no evidence of methylation for His74. (B) The *m/z* spectrum for the corresponding peptide purified from baculovirus shows evidence for methylation of His74 in the shifted size of the b5-H_2O ion (636.3 in methylated His74, arrow in B, vs 622.3 for nonmethylated His74, arrow in A). This result was confirmed by the corresponding differences in *m/z* for two additional ion series (b+2H and y+2H) (data not shown).

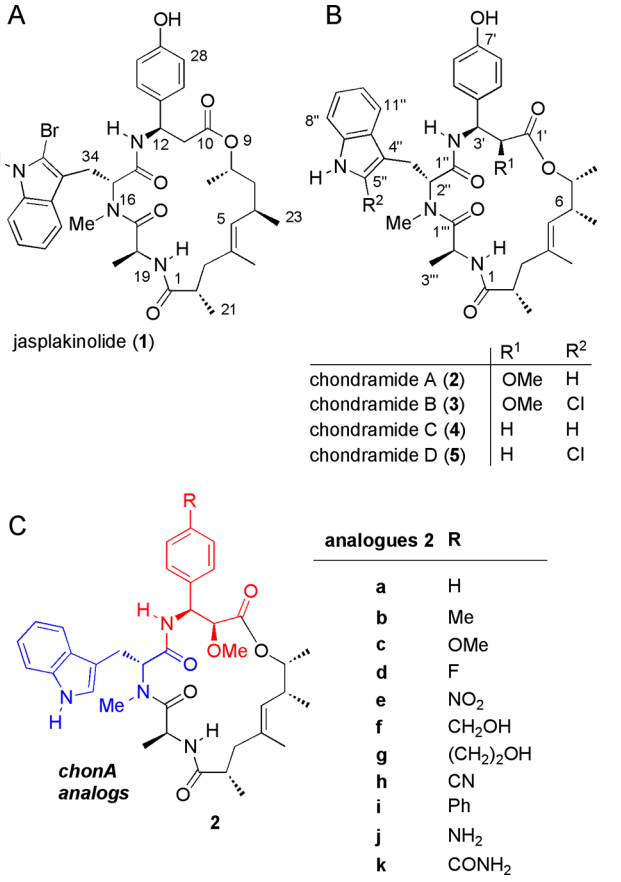

Figure 3. Structures of natural products and synthetic chondramides. (A) Diagram of jasplakinolide (**1**). (B) Diagrams of chondramides A, B, and C (**2**–**4**). (C) Diagrams of analogues of **2**. *β*-Tyrosine group is shown in red, and the *N*-methyl-D-tryptophan group is shown in blue.

both the steric and electrostatic properties of this side chain relative to mammalian actin. There are also differences in the proximity of the *N*-methyl-D-tryptophan moiety including amino acid changes from Lys270 to Met269 in muscle and Ala272 to Ser271 in muscle (Figure 1C,E). This former difference has previously been associated with enhanced fragility of the *T. gondii* F-actin filament.[20]

Testing of Natural Products and Synthetic Analogues. Jasplakinolide (**1**) and chondramides (**2**–**5**) each consist of a short hydroxy acid in a cyclic depsipeptide that contains the modified amino acids L-alanine, *N*-methyl-D-tryptophan, and L-*β*-tyrosine (Figure 3A,B). Compounds **2**–**4** differ in modifications at C-11 of the central lactam ring, where **2** and **3** have a methoxy group, while **4** has a hydrogen (Figure 3B). Additionally, **3** has a chlorine group at the C-5 position of the *N*-methyl-D-tryptophan, while **2** and **4** have a hydrogen (Figure 3B). We tested the activity of the natural products **1**–**4** on the growth of *T. gondii* parasites expressing *β*-galactosidase (*β*-gal) (Table 1, Figure 4). EC_{50} values were determined from the inhibition curves of *T. gondii* proliferation within confluent monolayers of HFF (human foreskin fibroblast) cells (Figure 4). Although some loss of monolayer confluency was observed at high concentrations of compounds, this did not prevent the measurement of EC_{50} values for parasite growth inhibition, which were consistently below these levels of toxicity (Figure 4). All four natural product compounds were potent in blocking growth, with EC_{50} values that ranged from ~0.2 to 0.7 *μ*M (Table 1). Both the natural product **2** and the synthetic product **2a** blocked *T. gondii* growth with similar potency, demonstrating that the synthetic products have comparable biological activity (Figure 4, Table 1).

Table 1. Biological Activities of Compounds[a]

compound	number	*T. gondii* EC_{50} (*μ*M)
Jas_np	**1**	0.34 ± 0.04
Chon A_np	**2**	0.56 ± 0.07
Chon B_np	**3**	0.22 ± 0.06
Chon C_np	**4**	0.48 ± 0.20
Chon A_syn	**2a**	0.51 ± 0.11
Chon A_CH_3	**2b**	0.53 ± 0.02
Chon A_OCH_3	**2c**	0.69 ± 0.15
Chon A_F	**2d**	0.32 ± 0.05
Chon A_NO_2	**2e**	0.61 ± 0.07
Chon A_CH_2OH	**2f**	0.74 ± 0.01
Chon A_CH_2CH_2OH	**2g**	0.60 ± 0.04
Chon A_CN	**2h**	0.38 ± 0.03
Chon A_Phenyl	**2i**	1.34 ± 0.05
Chon A_NH_2	**2j**	0.66 ± 0.02
Chon A_$CONH_2$	**2k**	≥45

[a]np = natural product (isolated), syn = synthetic compound.

We also took advantage of a series of analogues of **2** that have substitutions at the OH of the *β*-tyrosine group (Figure 2C)[45,47] and which might be expected to differentially affect parasite actin based on differences in this region of the actin-binding pocket described above. We compared a series of 10 synthetic derivatives (**2b**–**k**) for their ability to block parasite growth (Table 1). Several derivatives, notably chon A_F (**2d**) and chon A_CN (**2h**), were slightly more effective against *T.*

dx.doi.org/10.1021/np400196w | J. Nat. Prod. 2013, 76, 1565–1572

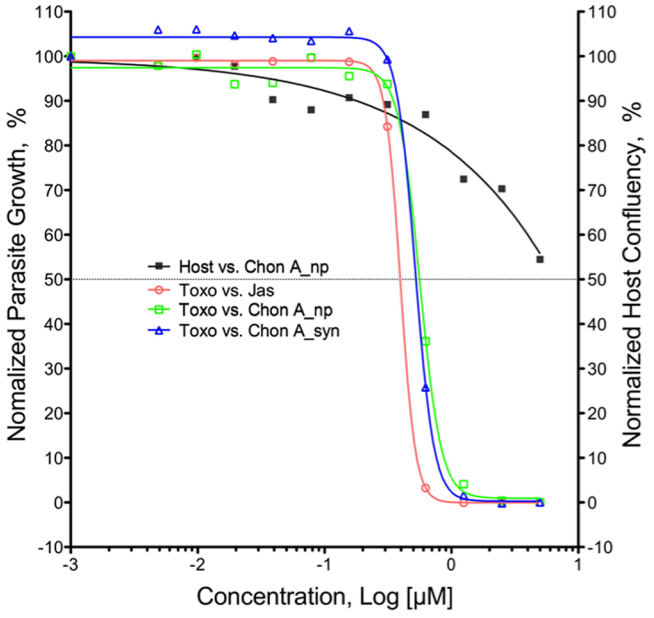

Figure 4. Inhibition of parasite growth by actin-stabilizing agents. Inhibition of *T. gondii* (Toxo) proliferation as determined by treating parasites expressing β-galactosidase (β-gal) with different concentrations of **1** (Jas), natural product **2** (Chon A_np), or synthetic **2a** (Chon A_syn) for 72 h. Normalized parasite growth inhibition curves from triplicates (left axis) were used to calculate EC_{50} values (see Table 1). HFF monolayer (host) confluency was determined using an MTS-based colorimetric assay after 72 h treatment with **2a** and normalized to the no treatment condition (right axis).

gondii when compared to the parent compound **2a** (Table 1). Introduction of a phenyl group decreased the potency for *T. gondii* by ~3-fold, suggesting this bulky side group is not well accommodated by the binding pocket (Table 1). Notably, substitution of NO_2 (**2e**), NH_2 (**2j**), or CH_2OH (**2g**) also decreased potency against the parasite (Table 1). The most dramatic change occurred with substitution with $CONH_2$ (**2k**), which eliminated activity against the parasite (Table 1).

On the whole, these synthetic analogues show a range of activities similar to the natural product **2**, but do not define significantly more potent inhibitors. These results also support the binding conformation described above, since modifications to the OH of the β-tyrosine of chondramide would be expected to fit in the pocket lined by Arg178, Asp179, and Gly200 (Figure 1B). In contrast, a previous model suggesting that the β-tyrosine of chondramide points toward Thr 202[46] is expected to have resulted in significant decreases in binding of the modified analogues. With the exception of **2k**, the affinities did not change dramatically (Table 1), leading us to favor the binding model proposed here. This same series of compounds has previously been used to examine growth inhibition of human cells, and they are also highly potent, with EC_{50} values ranging from 0.03 to 0.30 μM, with the exception of **2k**, which is much less potent (i.e., EC_{50} ~1.4 μM).[47]

Identification of Actin As the Molecular Target of Chondramides in *T. gondii*. Chondramides are thought to act similarly to **1** in stabilizing F-actin based on their phenotypic effects on host cells[41] and the ability to induce polymerization of mammalian actin *in vitro*.[44] However, the molecular differences in parasite actin also raise the possibility that while these compounds act to prevent infection, they may have a different molecular target in the parasite. To determine if inhibition of parasite growth was due to the modification of actin dynamics, we quantified the polymerization of TgACTI *in vitro*. Polymerization of 5 μM purified recombinant TgACTI was monitored in F-buffer supplemented with different concentrations of **1**, **2**, or **2a**, as described previously.[20] Light scattering increased with higher concentrations for all compounds tested, indicating that they promote actin polymerization (Figure 5). Compound **1** induced higher polymerization

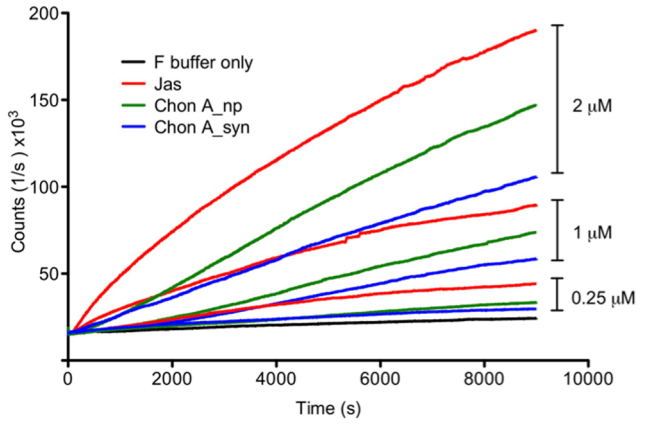

Figure 5. Jasplakinolide (**1**) and chondramide A (**2**, **2a**) induced dose-dependent polymerization of TgACTI *in vitro*. Ninety-degree light scattering was conducted to determine the kinetics of TgACTI polymerization in the presence of jasplakinolide (**1**) (Jas, red), natural product chondramide A (**2**) (Chon A_np, green), or synthetic chondramide A (**2a**) (Chon A_syn, blue). Polymerization of 5 μM TgACTI was induced by the addition of F-buffer containing DMSO (control, black) or different concentrations of the compounds: 0.25 μM, 1 μM, or 2 μM. The level of polymerization was monitored in counts per second over 9000 s.

compared to **2** or **2a** (Figure 5), suggesting it is more potent, a result consistent with its lower EC_{50} (Table 1). Compound **2** was slightly more efficient than **2a** in promoting TgACTI polymerization (Figure 4), even though the EC_{50} profile (Figure 4, Table 1) indicated almost identical potency between the two compounds. The dose-dependent polymerization of TgACTI by **2** and **2a** is consistent with their ability to block parasite invasion, as previously demonstrated with compound **1** on *T. gondii*.[34]

To further elucidate the mechanism of TgACTI modification by chondramide A (**2** and **2a**), we monitored the *in vitro* polymerization of parasite actin by phalloidin staining and visualization by fluorescence microscopy. Purified recombinant proteins were incubated with compound **1**, **2**, or **2a** in F-buffer supplemented with labeled phalloidin. F-actin filaments were evident even at relatively low concentrations of analogues (i.e., 0.25 μM, Figure 6A, left panels), corresponding to a molar ratio of 1:20. Interestingly, increasing the compound concentration to 2.0 μM led to formation of dense aggregates of actin filaments (Figure 6A, center panels). In the enlarged views, these aggregates appeared as clusters of very short filaments (Figure 6A, right panels). The length of F-actin filaments decreased from 15−20 μm at 0.25 μM to 7−10 μm at 2 μM of compounds (Figure 6B). This trend was consistent between **1** and both **2** and **2a**, suggesting a common mechanism of action and consistent with these compounds promoting assembly of actin, similar to previous reports on **1**.[30,31]

Chondramides Directly Affect Parasite Invasion. Previous studies have shown that chondramides, including

dx.doi.org/10.1021/np400196w | *J. Nat. Prod.* 2013, 76, 1565−1572

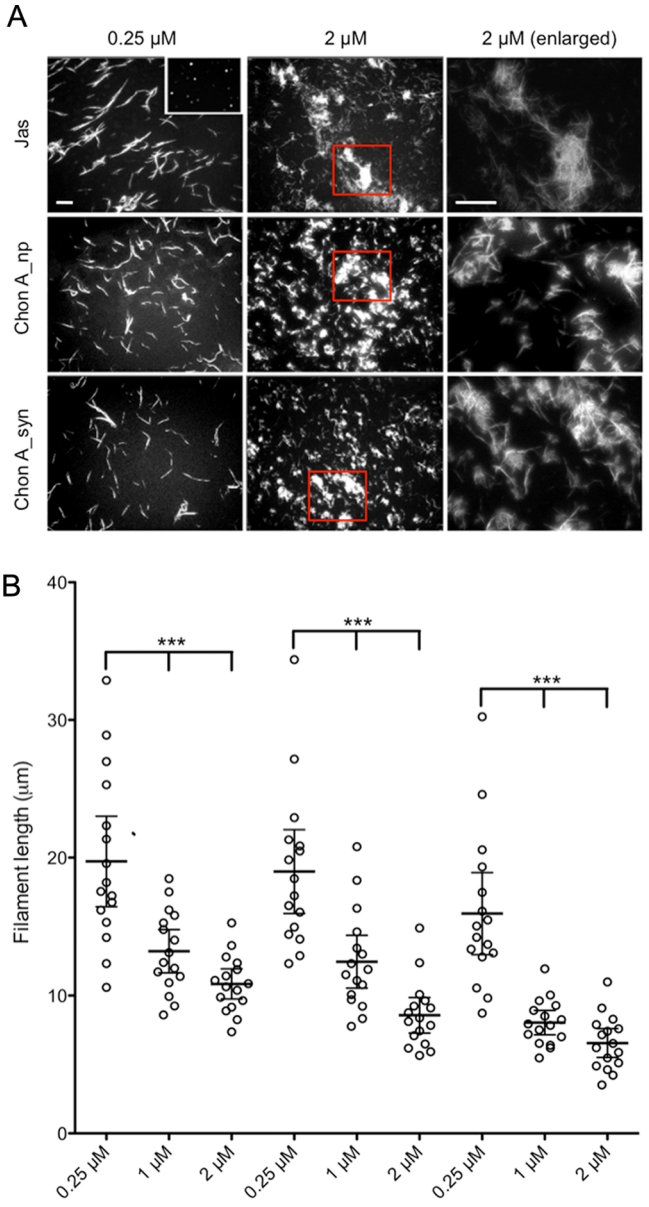

Figure 6. *In vitro* polymerization of TgACTI visualized by fluorescence microscopy of phalloidin-stained actin. (A) TgACTI (5 μM) was incubated in F-buffer for 1 h containing jasplakinolide (**1**) (Jas), natural product chondramide A (**2**) (Chon A_np), or synthetic chondramide A (**2a**) (Chon A_syn) at 0.25 μM (left panels) or 2 μM (center and right panels). Filaments were visualized by staining with 1.2 U/μL Alex 488 Fluor phalloidin. Enlarged areas from 2 μM treatments (red boxes) are shown in the far right panels. Scale bars = 10 μm. Inset: Negative control with no Jas or Chon A. (B) Determination of filament lengths from samples in A. Each data point represents an average of three filaments, as described in the Experimental Section. Means ± 95% CI. *** denotes significance using one-way ANOVA, $p < 0.0001$.

the analogues studied here, affect host cell replication, which is likely due to their effects on F-actin.[41,44,47] In contrast, the replication of *T. gondii* is independent of actin,[49] suggesting the observed effects of compounds in the growth assay are due to disruption of invasion, which is strongly dependent on actin-based motility in the parasite.[15,34] To test whether these compounds directly block invasion vs parasite growth, we compared the potency of **1** and **2a** during short-term treatment followed by washout vs continuous culture in the presence of compounds. EC_{50} values for compounds **1** and **2a** were only 1.5−2-fold higher in the short-term invasion assay followed by washout compared to continuous culture (Figure 7). Both **1**

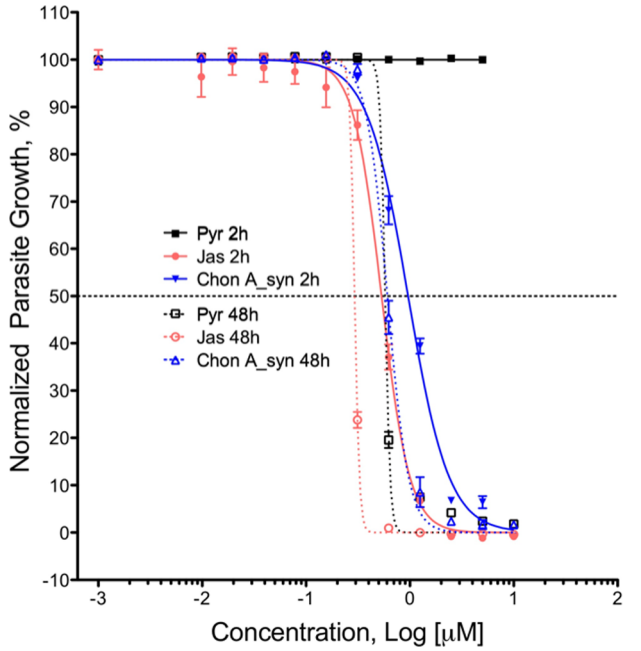

Figure 7. Inhibition of parasites expressing β-gal with different concentrations of pyrimethamine (Pyr), **1** (Jas), or **2a** (Chon A_syn) treated for 2 h followed by washout (solid lines) or treated continuously for 48 h (dashed lines). Normalized parasite growth inhibition curves ($n = 4$ replicates, mean ± SD) from a representative of three experiments with similar outcomes.

and **2a** were also significantly more potent in blocking subsequent parasite growth than pyrimethamine, a standard treatment for toxoplasmosis.[14] Pyrimethamine acts to block dihydrofolate reductase, disrupting folate metabolism, and requires at least 24 h of continuous treatment to affect parasite growth. In contrast, compounds **1** and **2a** act very rapidly by directly blocking parasite invasion into host cells. The slightly lower EC_{50} values seen during continuous culture suggested that these compounds also affect other functions during intracellular growth.

CONCLUSIONS

Our studies predict that actin is the primary molecular target of chondramides in *T. gondii*. Treatment of purified TgACTI *in vitro* induced polymerization of short clusters of filaments, indicating that these agents act directly on actin to induce filament formation. These results are consistent with chondramide having a similar mechanism of action to jasplakinolide (**1**), which has been reported to directly promote actin filament formation *in vitro* and disrupt filament turnover *in vivo*.[30,31] Similar to **1**, the binding of **2** to parasite actin stabilizes F-actin, resulting in disruption of motility and a block in cell invasion. Actin filaments are normally highly transient in *T. gondii*, and the parasite is thought to rely on rapid turnover of highly dynamic filaments. Consistent with this, genetic mutants that enhance stability of TgACTI filaments also disrupt motility and cell invasion.[20] Hence, chondramides and

dx.doi.org/10.1021/np400196w | *J. Nat. Prod.* 2013, 76, 1565−1572

jasplakinolide are natural products that target vulnerable and important processes in the parasite life cycle.

Although our findings indicate that subtle changes in the potency of chondramides can be achieved with modification of the OH group of the β-tyrosine, this did not give rise to compounds with notable improvement in potency against parasite actin. As well, these compounds have been shown in previous studies to disrupt mammalian actin and block cell division,[47] precluding their use for *in vivo* treatment at present. Modification to other regions of the chondramide scaffold, notably to the *N*-methyl-D-tryptophan moiety, would be the next logical step for generating compounds that might exploit differences in host and parasite actins, including differences at residues Lys270 and Ala272 (highlighted in yellow, Figure 1C and E), which correspond to Met269 and Ser271 in muscle. The previous description of an efficient method to generate analogues of **2a**[45,47] should facilitate generation of future compounds with modifications to the *N*-methyl-D-tryptophan moiety, alone or in combination with β-tyrosine analogues described here.

The chondramide derivatives described here may also be useful for probing the function of actin in other systems. For example, previous studies have shown that natural product chondramides (**2**−**5**) are active against fungal pathogens[43] and mammalian tumor cells.[41] The derivatives described here are likely to be active against these targets and may show greater potency than the natural products. Actin-based motility is also important in invasion of *Plasmodium*,[50] the causative agent of malaria, and *Cryptosporidium parvum*,[51] a common cause of diarrheal disease. Additionally, recent studies have emphasized the importance of actin in hemoglobin ingestion by *Plasmodium*[52,53] and in segregation of the apicoplast in *T. gondii*,[54] both unique functions not shared by their mammalian hosts. Hence, disruption of actin dynamics may provide a general strategy to disrupt multiple essential functions in parasites.

EXPERIMENTAL SECTION

General Experimental Procedures. Synthetic analogues of chondramide A were generated as previously reported including the total synthesis of a series of compounds that contain modified β-tyrosines.[45,47] Purity and confirmation of the identity of the compounds has been reported previously.[45,47]

Commercial and Natural Products. Jasplakinolide (**1**) was obtained from the marine sponge *Jaspis johnstoni* (Life Technology). Chondramides A, B, and C (**2**−**4**) were purified from *Chondramides crocatus*, as described previously,[41,43] provided by the Helmholtz Centre for Infection Research, Braunschweig, Germany. Compounds were dissolved in DMSO as stock solutions at 1 mM and stored at −20 °C until use. For use in biological experiments, compounds were diluted to final concentrations in Dulbecco's modified Eagle's medium supplemented with 10% fetal bovine serum and 10 μg/mL gentamicin (complete media) that also contained 0.2% DMSO.

Inhibition of *Toxoplasma gondii* Proliferation and EC_{50} Determination. *T. gondii* parasites expressing β-galactosidase (β-gal)[15] were incubated in complete media containing dilutions of compounds for 30 min and inoculated at 500 parasites/well in 96-well plates containing confluent HFF monolayers. Either parasites were cultured continuously in the presence of compounds, or the compounds were removed after 2 or 48 h by washing and returned to culture in complete medium (referred to as washout). After 72 h incubation at 37 °C and 5% CO_2, plates were washed in PBS, lysed by addition of 50 μL/well of lysis buffer (0.1 M HEPES pH8.0, 1 mM $MgSO_4$, 5 mM DTT, 1% Trion X-100), and incubated at 50 °C for 10 min. Assay buffer was added to each well (160 μL/well of 100 mM phosphate buffer pH 7.3, 102 mM β-mercaptoethanol, 9 mM $MgCl_2$) and incubated for 10 min at 37 °C. For β-gal substrate, 40 μL/well chlorophenol red-β-D-galactopyranoside (Boehringer Mannheim) was added and incubated for 10 min at 37 °C. Absorbance at 570 λ (A_{570}) was normalized to percentage of control (no treatment) and plotted against the $\log_{10}$ of compound concentrations using Prism 5.0 (GraphPad software). The $\log_{10}$ (inhibitor) vs response curve with variable slope was generated from three separate experiments (n = 4 replicates) to calculate EC_{50} values using Prism 5.0. To determine the effect of chondramide A (**2**) on host cell viability, confluent HFF monolayers were treated with serial dilutions of natural product chondramide A (**2**) for 72 h. The number of remaining viable cells was determined using the CellTiter 96 AQ_{ueous} One Solution cell proliferation assay (Promega) and analyzed in Prism 5.0 based on normalization vs untreated cells.

Actin Expression and Purification. N-Terminally His-tagged *T. gondii* actin (TgACTI) was purified on NiNTA agarose (Life Technology) from a baculovirus expression system using protocols described previously.[19] Purified protein was dialyzed overnight in G buffer (5 mM Tris-HCl, pH 8.0, 0.2 mM $CaCl_2$, 0.2 mM ATP) containing 0.5 mM DTT with 100 mM sucrose and clarified by centrifugation at 100000*g*, 4 °C, for 30 min to remove aggregates. Purified TgACTI was resolved on 12% SDS-PAGE gels followed by SYPRO Ruby (Molecular Probes) staining, visualized using a FLA-5000 phosphorimager (Fuji Film Medical Systems), and quantified using Image Gauge v4.23. TgACTI was stored at 4 °C and used within 2−3 days.

Ninety-Degree Light Scattering. Purified recombinant TgACTI was centrifuged at 100000*g*, 4 °C, for 30 min using a TL100 rotor and a Beckman Optima TL ultracentrifuge (Beckman Coulter) to remove aggregates. TgACTI was diluted to 5 μM in G buffer and placed in a 100 μL cuvette (submicro quartz fluorometer cell, Starna Cells). Light scattering was monitored with a PTI Quantmaster spectrofluorometer (Photon Technology International) at 310 nm (1 nm bandpass) for both excitation and emission at 21 °C. Once a steady reading was obtained, the acquisition was paused, and 1/10th volume of 10× F buffer (500 mM KCl, 20 mM $MgCl_2$, 10 mM ATP) was added to induce polymerization. Jasplakinolide (**1**), natural compound chondramide A (**2**), or synthetic chondramide A (**2a**) was added along with F-buffer to induce polymerization. The acquisition was restarted, and counts were collected for 9000 s.

Fluorescence Microscopy of Actin Filaments. Purified TgACTI was clarified of aggregates as described above and diluted to 5 μM in F-buffer (50 mM KCl, 2 mM $MgCl_2$, 1 mM ATP) with different concentrations of jasplakinolide (**1**) or chondramide A (**2**, **2a**). Alexa Fluor 488 phalloidin (Life Technology) was added at 1.2 U/μL to visualize actin filaments. After 1 h incubation, samples were placed on a slide and observed with a Zeiss Axioskop (Carl Zeiss) microscope using a 63× Plan-NeoFluar oil immersion lens (1.30 NA). Images were collected using a Zeiss Axiocam with Axiovision 3.1 and processed using linear adjustments in Adobe Photoshop CS4. Filament lengths were determined using the measurement feature of Axiovision software from 48 randomly selected filaments for each compound treatment. For graphing, data were plotted as the average of the three closest data points within each group. For statistical analysis, one-way ANOVA was performed in Prism 5.0 to compare data from different compound doses. Significant differences were defined as $p < 0.05$.

Molecular Dynamics Simulation and Docking. A model of skeletal alpha actin from *Homo sapiens* was created based on X-ray fiber diffraction data.[28] A 50 ns molecular dynamics (MD) simulation was carried out on this model using NAMD[55] with explicit waters and at a 50 mM salt concentration, as described previously.[20] Structural models for jasplakinolide (**1**) and chondramide A (**2**) were built using Maestro (Schrödinger LLC). Models were further optimized in continuum solvent using Jaguar (Schrödinger LLC), with the DFT level of theory using a hybrid B3LYP functional and 6-31G** basis set. A homology model for *T. gondii* F-actin was built using Modeler.[56] Docking was performed using Glide (Schrödinger LLC) to multiple snapshots taken at intervals of 200 ps from the 50 ns mammalian F-actin simulation. Default parameters were used for Glide.

Mass Spectrometry. Wild-type *T. gondii* (RH strain) parasites were lysed in NP-40 lysis buffer (1% NP-40, 100 mM NaCl, 50 mM Tris pH 8.0) at 4 °C for 2 h. Lysates were clarified by centrifugation at 2700*g*, 4 °C, for 5 min to remove nuclei. Actin was immunoprecipitated overnight by mouse anti-actin antibody clone C4 (Millipore) bound to Protein G Agarose beads (Thermo Scientific), following the commercial protocol for binding antibody to Protein G beads. Immunoprecipitated actin was eluted in 1% RapiGest SF reagent (Waters) with 20 mM DTT. TgACTI was also purified from baculovirus and kept in G buffer as described above. For mass spectrometry, both immunoprecipitated and purified actin were alkylated by iodoacetamide and diluted to 0.5% RapiGest SF reagent before overnight trypsin digestion. The samples were acidified with 0.5% trifluoroacetic acid and incubated at 37 °C for 45 min to remove RapiGest, then diluted with 5% acetonitrile/0.1% formic acid to give ∼0.5−1 pmol of actin per sample. Samples were analyzed by LC-MS/MS using an LTQ-Orbitrap Velos (Thermo Scientific) with a 1 h gradient. The data were searched using the MASCOT Distiller (Matrix Science, version 2.4.1) for post-translational modifications with a fragment ion mass tolerance of 0.80 Da and parent ion tolerance of 15 ppm.

■ ASSOCIATED CONTENT

Ⓢ Supporting Information

A stereopair image of the binding site of **2** with the TgACTI filament model is provided in Figure S1. This material is available free of charge via the Internet at http://pubs.acs.org.

■ AUTHOR INFORMATION

Corresponding Author

*E-mail: sibley@wustl.edu.

Author Contributions

The manuscript was written through contributions of all authors. All authors have given approval to the final version of the manuscript.

Notes

The authors declare no competing financial interest.

■ ACKNOWLEDGMENTS

We are grateful to Dr. R. Jansen, Helmholtz Centre for Infection Research, for providing the chondramide natural products, Dr. K. Skillman for advice on actin polymerization assays, and S. Alvarez for performing the mass spectrometry. This work was supported by a grant from the National Institutes of Health (AI073155).

■ REFERENCES

(1) Hall, S.; Ryan, K. A.; Buxton, D. The epidemiology of toxoplasma infection. In *Toxoplasmosis: A Comprehensive Clinical Guide*; Joynson, D. H.; Wreghitt, T. J., Eds.; Cambridge University Press, 2001; pp 58−124.

(2) Pfaff, A. W.; Liesenfeld, O.; Candolfi, E., Congenital toxoplasmosis. In *Toxoplasma: Molecular and Cellular Biology*; Ajioka, J. W.; Soldati, D., Eds.; Horizon Bioscience: Norfolk, 2007; pp 93−110.

(3) Israelski, D. M.; Remington, J. S. *Curr. Clin. Top. Infect. Dis.* **1993**, *13*, 322−356.

(4) Mariuz, P.; Steigbigel, R. T. Toxoplasma infection in HIV-infected patients. In *Toxoplasmosis a Comprehensive Clincial Guide*; Joynson, D. H. M.; Wreghitt, T. G., Eds.; Cambridge Univ. Press: Cambridge, 2007; pp 147−177.

(5) Balogou, A. A.; Saka, B.; Kombate, D.; Kombate, K.; Mouhari-Toure, A.; Akakpo, S.; Singo, A.; Pitche, P. *Trop. Doct.* **2011**, *41*, 215−7.

(6) Biggs, B.; Hewish, M.; Kent, S.; Hayes, K.; Crowe, S. *J. Immunol.* **1995**, *154*, 6132−6139.

(7) Bouckenooghe, A. R.; Shandera, W. X. *J. Immigr. Health* **2002**, *4*, 81−86.

(8) Dennis, A. M.; Napravnik, S.; Sena, A. C.; Eron, J. J. *Clin. Infect. Dis.* **2011**, *53*, 480−487.

(9) Oliveira, J. F.; Greco, D. B.; Oliveira, G. C.; Christo, P. P.; Guimaraes, M. D.; Oliveira, R. C. *Rev. Soc. Bras. Med. Trop.* **2006**, *39*, 146−151.

(10) Oshinaike, O. O.; Okubadejo, N. U.; Ojini, F. I.; Danesi, M. A. *Nig. Q. J. Hosp. Med.* **2010**, *20*, 104−107.

(11) Glasner, P. D.; Silveira, C.; Kruszon-Moran, D.; Martins, M. C.; Burnier, M.; Silveira, S.; Camargo, M. E.; Nussenblatt, R. B.; Kaslow, R. A.; Belfort, R. *Am. J. Opthalmol.* **1992**, *114*, 136−144.

(12) Jones, L. A.; Alexander, J.; Roberts, C. W. *Parasite Immunol.* **2006**, *28*, 635−642.

(13) Roberts, F.; Mets, M. B.; Ferguson, D. J.; O'Grady, R.; O'Grady, C.; Thulliez, P.; Brezin, A. P.; McLeod, R. *Arch. Ophthalmol.* **2001**, *119*, 51−58.

(14) McCabe, R. E. Antitoxoplasma chemotherapy. In *Toxoplasmosis: a Comprehensive Clinical Guide*; Joynson, D. H. M.; Wreghitt, T. G., Eds.; Cambridge Univ. Press: Cambridge, 2001; pp 319−359.

(15) Dobrowolski, J. M.; Sibley, L. D. *Cell* **1996**, *84*, 933−939.

(16) Gonzalez, V.; Combe, A.; David, V.; Malmquist, N. A.; Delorme, V.; Leroy, C.; Blazquez, S.; Menard, R.; Tardieux, I. *Cell Host Microbe* **2009**, *5*, 259−272.

(17) Sibley, L. D. *Curr. Opin. Biotechnol.* **2010**, *21*, 592−598.

(18) Baum, J.; Papenfuss, A. T.; Baum, B.; Speed, T. P.; Cowman, A. F. *Nat. Rev. Microbiol.* **2006**, *4*, 621−628.

(19) Sahoo, N.; Beatty, W. L.; Heuser, J. E.; Sept, D.; Sibley, L. D. *Mol. Biol. Cell* **2006**, *17*, 895−906.

(20) Skillman, K. M.; Diraviyam, K.; Khan, A.; Tang, K.; Sept, D.; Sibley, L. D. *PLoS Pathogens* **2011**, *7*, e1002280.

(21) Mehta, S.; Sibley, L. D. *J . Biol. Chem.* **2010**, *285*, 6835−6847.

(22) Mehta, S.; Sibley, L. D. *Mol. Biol. Cell* **2011**, *22*, 1290−1299.

(23) Skillman, K. M.; Daher, W.; Ma, C.; Soldati-Favre, D.; Sibley, L. D. *Biochemistry* **2012**, *51*, 2486−2495.

(24) Schüler, H.; Matuschewski, K. *Traffic* **2006**, *7*, 1433−1439.

(25) Dobrowolski, J. M.; Niesman, I. R.; Sibley, L. D. *Cell Motil. Cytoskel.* **1997**, *37*, 253−262.

(26) Schmitz, S.; Grainger, M.; Howell, S. A.; Calder, L. J.; Gaeb, M.; Pinder, J. C.; Holder, A. A.; Veigel, C. *J. Mol. Biol.* **2005**, *349*, 113−125.

(27) Aikawa, M.; Miller, L. H.; Johnson, J.; Rabbege, J. *J. Cell Biol.* **1978**, *77*, 72−82.

(28) Oda, T.; Namba, K.; Maeda, Y. *Biophys. J.* **2005**, *88*, 2727−2736.

(29) Crews, P.; Manes, L. V.; Boehler, M. *Tetrahedron Lett.* **1986**, *27*, 2797−2800.

(30) Bubb, M. R.; Senderowicz, A. M.; Sausville, E. A.; Duncan, K. L.; Korn, E. D. *J. Biol. Chem.* **1994**, *269*, 14869−14871.

(31) Bubb, M. R.; Spector, I.; Beyer, B. B.; Fosen, K. M. *J. Biol. Chem.* **2000**, *275*, 5163−5170.

(32) Poupel, O.; Tardieux, I. *Microbes Infect.* **1999**, *1*, 653−662.

(33) Shaw, M. K.; Tilney, L. G. *Proc. Natl. Acad. Sci. U.S.A.* **1999**, *96*, 9095−9099.

(34) Wetzel, D. M.; Hakansson, S.; Hu, K.; Roos, D.; Sibley, L. D. *Mol. Biol. Cell* **2003**, *14*, 396−406.

(35) Hayot, C.; Debeir, O.; Van Ham, P.; Van Damme, M.; Kiss, R.; Decaestecker, C. *Toxicol. Appl. Pharmacol.* **2006**, *211*, 30−40.

(36) Scott, V. R.; Boehme, R.; Matthews, T. R. *Antimicrob. Agents Chem.* **1988**, *32*, 1154−1157.

(37) Senderowicz, A. M.; Kaur, G.; Sainez, E.; Laing, C.; Inamn, W. D.; Rodriguez, J.; Crews, P.; Malspeis, L.; Grever, M. R.; Sausville, E. A. *J. Natl. Cancer Inst.* **1995**, *87*, 46−51.

(38) Takeuchi, H.; Ara, G.; Sausville, E. A.; Teicher, B. *Cancer Chemother. Pharmacol.* **1998**, *42*, 491−496.

(39) Cramer, L. P. *Curr. Biol.* **1999**, *9*, 1095−1105.

(40) Watts, K. R.; Morinaka, B. I.; Amagata, T.; Robinson, S. J.; Tenney, K.; Bray, W. M.; Gassner, N. C.; Lokey, R. S.; Media, J.; Valeriote, F. A.; Crews, P. *J. Nat. Prod.* **2011**, *74*, 341−351.

(41) Sasse, F.; Kunze, B.; Gronewold, T. M. A.; Reichenbach, H. *J. Natl. Cancer Inst.* **1998**, *90*, 1559−1563.
(42) Holzinger, A.; Lutz-Meindl, U. *Cell Motil. Cytoskel.* **2001**, *48*, 87−95.
(43) Kunze, B.; Jansen, R.; Sasse, F.; Höfle, G.; Reichenbach, H. *J. Antibiot. (Tokyo)* **1995**, *48*, 1262−1266.
(44) Eggert, U.; Diestel, R.; Sasse, F.; Jansen, R.; Kunze, B.; Kalesse, M. *Angew. Chem., Int. Ed.* **2008**, *47*, 6478−6482.
(45) Schmauder, A.; Sibley, L. D.; Maier, M. E. *Chem.−Eur. J.* **2010**, *16*, 4328−4336.
(46) Waldmann, H.; Hu, T. S.; Renner, S.; Menninger, S.; Tannert, R.; Oda, T.; Arndt, H. D. *Angew. Chem., Int. Ed.* **2008**, *47*, 6473−6477.
(47) Zhdanko, A.; Schmauder, A.; Ma, C. I.; Sibley, L. D.; Sept, D.; Sasse, F.; Maier, M. E. *Chem.−Eur. J.* **2011**, *17*, 13349−13357.
(48) Lorenz, M.; Popp, D.; Holmes, K. C. *J. Mol. Biol.* **1993**, *234*, 826−836.
(49) Shaw, M. K.; Compton, H. L.; Roos, D. S.; Tilney, L. G. *J. Cell Sci.* **2000**, *113* (Pt. 7), 1241−1254.
(50) Baum, J.; Richard, D.; Healer, J.; Rug, M.; Krnajski, Z.; Gilberger, T. W.; Green, J. L.; Holder, A. A.; Cowman, A. F. *J. Biol. Chem.* **2006**, *281*, 5197−5208.
(51) Wetzel, D. M.; Schmidt, J.; Kuhlenschmidt, M.; Dubey, J. P.; Sibley, L. D. *Infect. Immun.* **2005**, *73*, 5379−5387.
(52) Lazarus, M. D.; Schneider, T. G.; Taraschi, T. F. *J. Cell Sci.* **2008**, *121* (Pt 11), 1937−1949.
(53) Smythe, W. A.; Joiner, K. A.; Hoppe, H. C. *Cell. Microbiol.* **2008**, *10*, 452−464.
(54) Andenmatten, N.; Egarter, S.; Jackson, A. J.; Jullien, N.; Herman, J. P.; Meissner, M. *Nat. Methods* **2012**, *10*, 125−127.
(55) Kale, L.; Skeel, R.; Bhandarkar, M.; Brunner, R.; Gursoy, A.; Krawetz, N.; Phillips, J.; Shinozaki, A.; Varadarajan, K.; Schulten, K. *J. Comp. Phys.* **1999**, *151*, 283−312.
(56) Martí-Renom, M. A.; Stuart, A. C.; Fiser, A.; Sánchez, R.; Melo, F.; Sali, A. *Annu. Rev. Biophys. Biomol. Struct.* **2000**, *29*, 291−325.